Available online at www.sciencedirect.com
SCIENCE DIRECT®
Biochemical and Biophysical Research Communications 338 (2005) 423–431
BBRC
www.elsevier.com/locate/ybbrc

Review

Renal localization, expression, and developmental regulation of P450 4F cytochromes in three substrains of spontaneously hypertensive rats ☆

Auinash Kalsotra [a], Xiaoming Cui [a,b], Sayeepriyadarshini Anakk [a], Cruz A. Hinojos [c], Peter A. Doris [c], Henry W. Strobel [a,*]

[a] *Department of Biochemistry and Molecular Biology, Medical School at Houston, Schering-Plough Research Institute, Kenilworth, NJ 07033, USA*
[b] *Drug Metabolism and Safety, Schering-Plough Research Institute, Kenilworth, NJ 07033, USA*
[c] *Institute of Molecular Medicine, University of Texas HSC at Houston, USA*

Received 27 July 2005
Available online 25 August 2005

Abstract

Cytochrome P450 4F isoforms have been shown to metabolize arachidonic acid to generate 20-hydroxyeicosatetraenoic acid (20-HETE), a potent eicosanoid that modulates vascular tone and renal tubular function. 20-HETE production in the kidney is implicated in the development of essential hypertension in the spontaneously hypertensive rat (SHR). In this study, we determined CYP4F mRNA localization and distribution in rat liver and kidney by in situ hybridization and real time quantitative PCR. CYP4Fs are regionally distributed in the kidney with CYP4F1, 4F4, and 4F5 being expressed more in the renal cortex than medulla while CYP4F6 shows higher medullary expression. We investigated developmental CYP4F gene expression in three different substrains of SHR. Distinct age-dependent patterns of expression were seen for individual CYP4F isoforms in Wistar–Kyoto (WKY) and three SHR substrains (B2, C, and A3). A steady increase in CYP4F1 expression with age was seen in each of the three substrains which correlate well with increased 20-HETE levels and elevated blood pressure seen in these animals. CYP4F4 expression increased significantly at 8 weeks followed by a precipitous fall in WKY and A3 strains at 12 weeks of age. In strains B2 and C, CYP4F4 levels started declining as early as 8 weeks of age. CYP4F5 and 4F6 levels fluctuated with age in a biphasic manner with a different profile for each sub-strain. Based on the expression profile and catalytic activity, CYP4F1 seems to be the most critical 4F isoform involved in the production of 20-HETE in the SHR kidney.

Keywords: Cytochrome P450 4F; SHR; 20-HETE; Kidney

20-Hydroxyeicosatetraenoic acid (20-HETE) is an ω-hydroxylated derivative and a major metabolite of arachidonic acid (AA) produced in the kidney of several species, including humans [1]. It is known to regulate renal vascular tone [2,3], inhibit Na^+/K^+-ATPase [4] and the 70-ps K^+ channel in the medullary thick ascending limb [5], auto-regulate renal blood flow and glomerular filtration rate [6], and cause dose-dependent vasoconstriction of renal arcuate arteries [7]. Alterations in renal 20-HETE production may also contribute to the development of hypertension in both the spontaneously hypertensive rat (SHR) [8–10] and the Dahl salt-sensitive (Dahl S) rat [11].

20-HETE is primarily produced by the members of cytochrome P450 (CYP) 4 family. The *CYP4A* subfamily was the first to be characterized to catalyze AA ω-hydroxylation but recently the *CYP4F* subfamily has been shown to be equally important in AA metabolism [12]. There are four CYP4A and four 4F isoforms in the rat, three 4As and five 4Fs in mice, and two 4As and five 4Fs in humans [12–14]. CYP4A11 is the major human CYP4A isoform and CYP4A11 purified from both liver and kidney is able to carry out both ω and ω-1 hydroxylation of AA

☆ *Abbreviations: CYP* and P450, cytochrome P450; LTB_4, leukotriene B_4; HETE, hydroxyeicosatetraenoic acid; SHR, spontaneously hypertensive rat; WKY, Wistar–Kyoto; QRTPCR, quantitative real time PCR.

* Corresponding author. Fax: +1 713 500 0652.
E-mail address: henry.w.strobel@uth.tmc.edu (H.W. Strobel).

0006-291X/$ - see front matter © 2005 Elsevier Inc. All rights reserved.
doi:10.1016/j.bbrc.2005.08.101

[15,16]. However, in both studies, CYP4F2-catalyzed 20-HETE formation was shown to be quantitatively more important than CYP4A11. Although most CYP4Fs have a common feature of metabolizing leukotriene B_4 (LTB_4) a pro-inflammatory molecule, considerable differences in their substrate specificities exist. For instance, CYP4F3B, a liver-specific splice variant of *CYP4F3* gene, also metabolizes AA to 20-HETE quite significantly [17].

In rats, CYP4A1 is the most active isoform to metabolize AA followed by 4A2/4A3 and 4A8 with respective K_{cat} values of 6, 2, and 1 min^{-1} [18,19]. Recently, Xu et al. [20] conducted a direct comparison of the four rat CYP4F isoforms for their ability to metabolize AA. CYP4F1 and 4F4 were identified as major catalysts for 20-HETE formation and the K_{cat} values for CYP4F1 (9 min^{-1}) and 4F4 (11 min^{-1}) were found to be quite similar to what was reported for CYP4A isoforms [18]. We have shown previously that CYP4F isoforms are expressed abundantly in rat kidney both at the mRNA and protein levels [21], which strengthens the argument that in an in vivo setting, CYP4Fs may be playing an equivalent role as CYP4As in 20-HETE generation.

SHR is an inbred rat model of heritable essential hypertension. SHR exists in several substrains, differing principally in susceptibility to hypertensive end organ injury [22]. Intercrosses between SHR substrains indicate a common genetic basis of hypertension among them [23,24]. Increased arachidonic acid ω-hydroxylase activity has been documented in the SHR kidney relative to the normotensive Wistar–Kyoto (WKY) rat, suggesting that increased renal 20-HETE levels contribute to the hypertensive phenotype in these rats [9,25–27]. Increases in CYP4A mRNA and protein levels have been seen in the SHR kidney that are consistent with the increased arachidonic acid ω-hydroxylase activity; however, the mechanism of altered CYP4A expression remains unknown [9]. Furthermore, CYP4A3 and 4A8 expression was suggested to be critical in the early changes in eicosanoid formation and renal function in the young spontaneously hypertensive rat.

In this study, we first determined the localization of CYP4Fs in liver and kidney by in situ RNA hybridization and real time quantitative PCR. Second, we investigated their developmental expression in three different substrains of SHR at different ages. Finally, based on CYP4F catalytic properties, an effort was made to correlate the expression pattern with the hypertensive phenotype in these animals.

Materials and methods

Materials. Restriction enzymes, T4 DNA ligase, and *Taq* DNA polymerase were purchased from Invitrogen Life Technologies (Carlsbad, CA). All reagents used were of analytical grade or higher.

Animals and tissue collection. Six- to eight-week-old male Wistar rats (Harlan, Indianapolis, IN) were used for in situ hybridization studies and QRTPCR analysis (see below). The animals were allowed free access to food and water at all times. The animals were killed 24 h after treatments by CO_2 asphyxiation. The livers and kidneys were removed for RNA preparation.

Transcript profiling studies were performed on 4-, 8-, 12-, and 18-week-old male animals. We used normotensive Wistar–Kyoto (WKY) and SHR-A3 rats of the Heidelberg sub-strains that have been maintained in our facility for 8 years. SHR-B2 and SHR-C animals were descended from stocks maintained in our facility and originally provided by Professor T. Suzuki, Kinki University School of Medicine, Kinki, Japan. The genealogy of these sub-strains has been previously described [22]. Blood pressure phenotypes of these strains are verified in our colony. All animals used in the studies were produced in our breeding program and housed under controlled conditions in an AAALAC-approved animal facility. Animals were provided a standard rodent chow diet and drinking water ad libitum.

Animals were anesthetized by isoflurane inhalation and kidneys were rapidly dissected via ventral laparotomy to harvest kidney for RNA used in QRTPCR studies. Renal gene expression analysis was performed using total RNA preparations from axial renal segments including cortex and medulla. Ureteric pelvis and major vascular structures of the renal sinus were removed from the sample. Three or four animals from each strain were used at each time point to permit all gene expression measurements to be statistically analyzed. Each sample from each animal was treated as an independent sample and no pooling was performed.

All animal procedures were approved by Animal Care and Use Committee of The University of Texas HSC at Houston.

In situ hybridization. Rats were killed, and the livers and kidneys were removed, cut open and washed with cold phosphate-buffered saline (PBS) immediately. The tissues were fixed with 4% paraformaldehyde in PBS overnight at 4 °C with gentle rocking. The samples were dehydrated with 30% ethanol in PBS, 50% ethanol in PBS, 70% ethanol in H_2O, 85% ethanol in H_2O, 95% ethanol in H_2O, and 100% ethanol. After clearing the sample with a 1:1 mixture of ethanol and histoclear (Fisher Scientific), and then 100% histoclear, the samples were infiltrated with paraffin and histoclear (50:50) followed by 3×30 min in 100% paraffin at 65 °C. Embedding was carried out with 100% paraffin at room temperature. The embedded samples were sectioned on a rotary microtome and mounted onto glass slides. In situ hybridization was performed with [^{35}S-UTP]-labeled riboprobes on these slides. 1×10^6 cpm probe was used on each slide. The slides were placed on X-ray film for 3 days to determine exposure time. Afterwards, they were dipped in NBT2 nuclear emulsion and kept desiccated in the dark at room temperature for 4 or 5 days. The slides were developed and counterstained with Hoechst 33258 and examined under a microscope with UV epifluoresence and a red light source to view nuclei and silver grains simultaneously.

RNA probes. The DNA fragments for CYP4F4 and 4F5 RNA probes were amplified by PCR using the full-length cDNA clones in pBluescript as templates. The forward primer (Linker:5′-GCT CTA GAA CTA GTG GAT C-3′) was designed to anneal to the vectors just upstream of the 5′-end of cDNAs, and the reverse primers (4F4 in situ: 5′-CTC GAG GTT GAG GGA AAT CAC A-3′) (4F5 in situ: 5′-CTC GAG TGC CTT CCT CAT TGC T-3′) are specific for 4F4 and 4F5 cDNA sequences. The resulting 300 bp of CYP4F4 and 291 bp of CYP4F5 PCR fragments were ligated into TA vector. The *Pst*I–*Xho*I fragments from TA vector were further subcloned into the pBluescript KS vector. [^{35}S-UTP]-labeled antisense and sense probes for CYP4F4 and CYP4F5 were synthesized with the T7 or T3 RNA polymerase, after the plasmids were linearized with *Pst*I or *Xho*I, respectively. The specific activities of ^{35}S-UTP probes were approximately 1 to 3×10^7 cpm/μg.

RNA preparation and quantitative real time PCR (QRTPCR). Total RNA was prepared according to the method of Chomczynski and Sacchi [28]. All samples were DNAse treated using RQ1 DNAse (Promega, Madison, WI). The quality of the isolated RNA was assessed by electrophoresis on 1% agarose gels based on the integrity of 28S and 18S bands after ethidium bromide staining. PCR primers and fluorescent probe sequences for CYP4F isoforms were designed as described previously [21]. Aliquots (200 ng) of total RNA were reverse-transcribed in quadruplicate (including an RT blank to account for amplification of contaminating genomic DNA). Amplification was performed using an ABI Prism 7700 (Applied Biosystems, Norwalk, CT) at 95 °C for 1 min, followed by 40

cycles of 95 °C for 12 s and 60 °C for 1 min. Standard curves were generated by plotting C_t versus the log of the amount of amplicons (custom made from IDT, Coralville, IA) for specific 4F (500 ag–5 pg) and were used to compare the relative amount of a particular CYP4F mRNA in the samples.

Statistical analysis. Results are expressed as means ± SEM from at least five independent sets of experiments. Comparisons were made using Student's *t* test and one-way analysis of variance with a post hoc Tukey's multiple range test. Values of $P < 0.05$ were considered statistically different.

Results

Localization of CYP4F4 and CYP4F5 in rat liver and kidney

In situ hybridization was performed to determine the regional distribution pattern of CYP4F4 and CYP4F5 in rat liver and kidney. For these studies, RNA probes were synthesized from the first 291 and 300 bp of CYP4F4 and CYP4F5 cDNAs, respectively. These probes contain the whole 5′UTR region and the 5′ termini of the coding regions which are the least homologous regions among all rat CYP4F coding sequences. This gives a less than 55% sequence homology between these two RNA probes, which is sufficient to differentiate between 4F4 and 4F5 expression with the in situ hybridization conditions we used. The sense RNA probes were used to control non-specific hybridization signals (Figs. 1a, 2a and b).

In liver, both 4F4 and 4F5 were expressed ubiquitously in the central lobular and para-ventricular regions. Under the same exposure time, 4F4 showed a signal stronger than that of 4F5 (Fig. 1a). Similar expression profiles for 4F4 and 4F5 were obtained by real time PCR analysis (Fig. 1b). In kidney, intense 4F5 hybridization signals were observed in the cortex and outer medullary regions where proximal tubules predominate. Interestingly, 4F4 signal in kidney was much weaker than 4F5 as seen by both in situ and real time PCR (Figs. 2a–c). Very low expression for both 4F4 and 4F5 was observed in the inner medullary region containing the loops and collecting tubules. Also, the glomeruli did not show any 4F4 or 4F5 expression (Fig. 2, lower panels of a and b).

QRTPCR offers increased sensitivity and specificity to compare localization or discern differences in the relative expression of CYP4F isoforms in the rat kidney. This is in part due to the smaller size of amplicons (<100 bp long) generated by QRTPCR reaction vs. the larger probe size (>300 bp long) required for in situ determinations. In localization studies using RNA prepared from individually dissected renal cortex and medulla, preferential cortical expression was seen for CYP4F1, 4F4, and 4F5 (Fig. 3). Compared to the medulla, the cortex had 2-, 2.5-, and 2.2-fold higher expression of CYP4F1, 4F4, and 4F5, respectively. In contrast, 4F6 was expressed 1.7-fold higher in medulla than in cortex (Fig. 3).

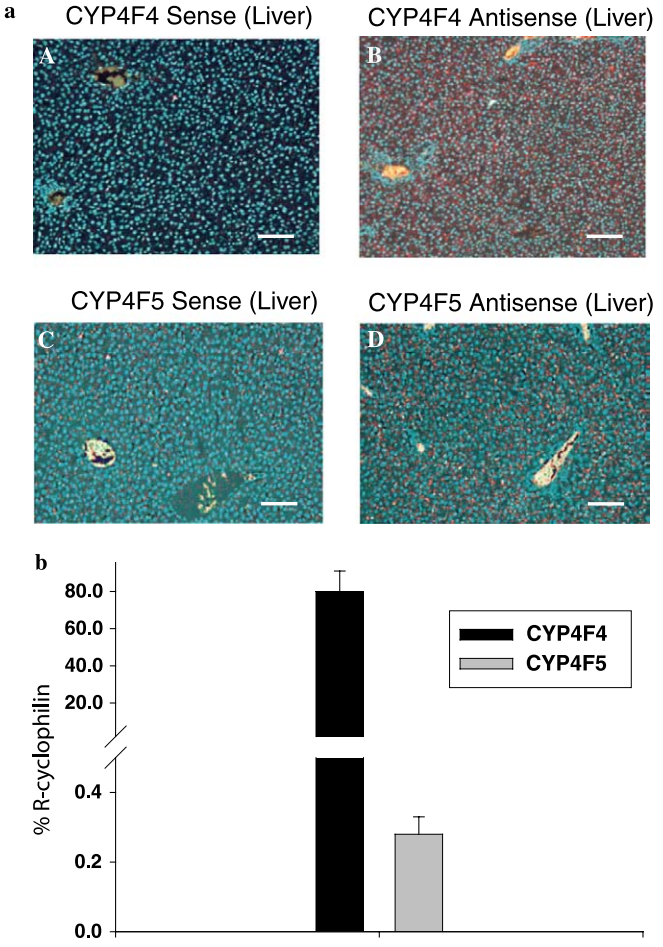

Fig. 1. (a) Localization of CYP4F4 and CYP4F5 mRNA by in situ hybridization in rat liver. The liver sections were hybridized either to 4F4 antisense (panel B) or 4F5 antisense (panel D) ^{35}S RNA probes. For negative controls, panel A was hybridized with 4F4 sense probe, panel C with 4F5 sense probe. Red represents the hybridization signals. Blue represents cell nuclei. Orange represents blood in blood vessel. Bars = 50 μm (b). Quantitative real time PCR analysis of CYP4F4 and 4F5 expression in rat liver. Total RNA from rat liver ($n = 4$) was prepared and each sample was assayed in quadruplicates using QRTPCR as described in Materials and methods. All data were normalized to r-cyclophilin. Values are expressed as means ± SE.

Developmentally regulated expression of CYP4F isoforms in renal tissue

WKY rats

Distinct developmental patterns of expression in the kidney were detected for individual CYP4F genes, as illustrated in Table 1. The expression of r-cyclophilin gene showed no evidence of either strain- or age-related differences and was therefore accepted as an appropriate control. In WKY rats, CYP4F4 levels doubled at 8 weeks but thereafter declined sharply by 12 and 16 weeks of age. 4F5 expression also decreased by 50% at 12–18 weeks when compared with 4 weeks expression. 4F6 levels, in contrast, increased by 40% at 8 weeks and 4-fold by 12 weeks of age. However, at 18 weeks 4F6 levels were reduced back to their 4 weeks

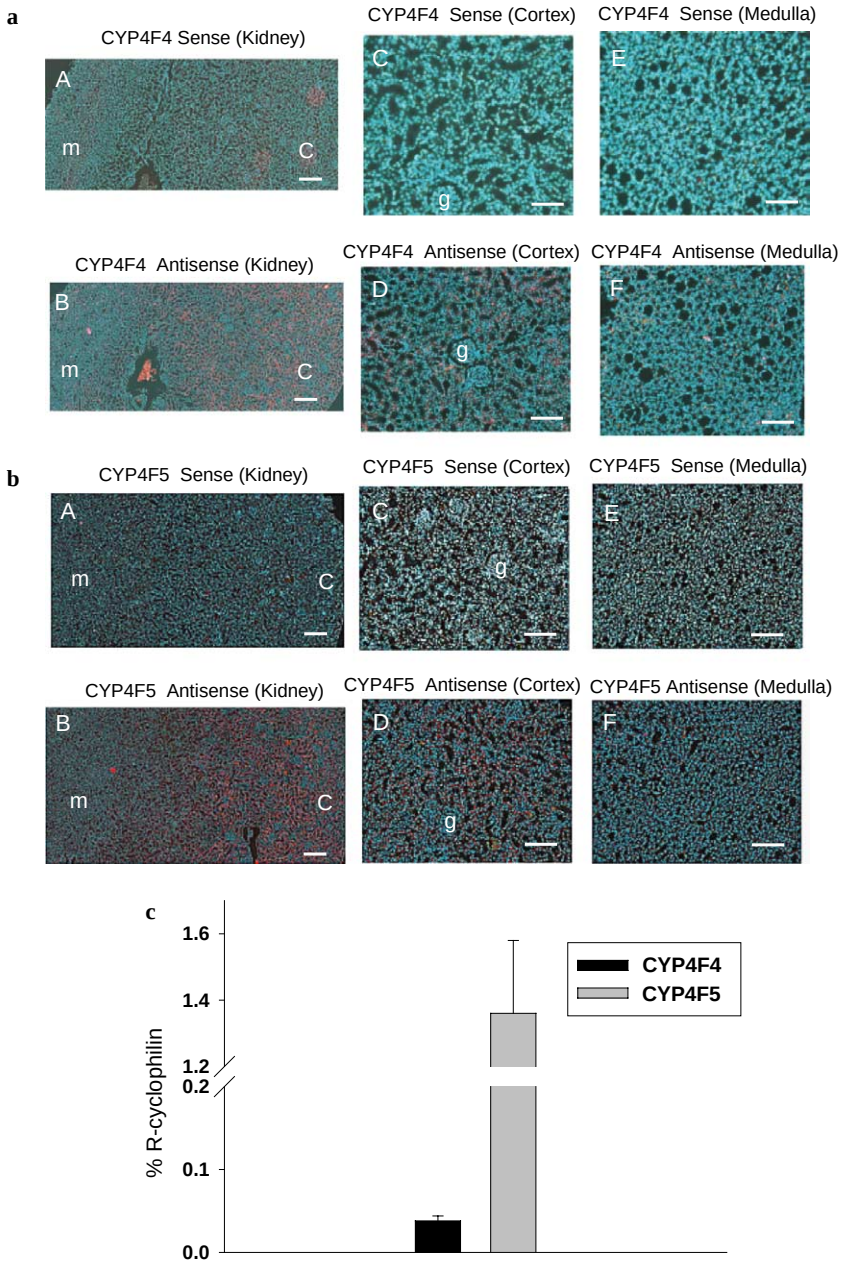

Fig. 2. (a) Localization of CYP4F4 mRNA by in situ hybridization in rat kidney. The transverse kidney sections were hybridized to 4F4 anti-sense probes (panel B). 4F4 sense probe was used as a control for nonspecific background (panel A) Bars = 100 μm. Cortex (C,D) and medulla (E,F) were visualized with higher magnitude (bars = 20 μm). Panels C,E represent cortex region were hybridized with sense and panels D,F were hybridized to anti-sense 4F4 probes. Red represents the hybridization signals; blue represents the nuclei. g, m, and c indicate the glomeruli, medulla and cortex region. (b) Localization of CYP4F5 mRNA by in situ hybridization in rat kidney. The transverse kidney sections were hybridized to 4F5 anti-sense probes (panel B). 4F5 sense probe was used as a control for nonspecific background (panel A) bars = 100 μm. Cortex (C,D) and medulla (E,F) were visualized with higher magnitude (bars = 20 μm). Panels C,E were hybridized with sense and panels D,F were hybridized to anti-sense 4F4 probes. Red represents the hybridization signals; blue represents the nuclei. g, m, and c indicate the glomeruli, medulla, and cortex region. (c) Quantitative real time PCR analysis of CYP4F4 and 4F5 expression in rat kidney. Total RNA from rat kidney ($n = 4$) was prepared and each sample was assayed in quadruplicate using QRTPCR as described in Materials and methods. All data were normalized to r-cyclophilin. Values are expressed as means ± SE.

levels. No significant change in 4F1 expression was observed with respect to age in WKY rats.

SHR-B2

In the SHR-B2, CYP4F1 mRNA expression increased steadily with age. 4F1 expression increased by 2.2-fold in 8 week olds, 2.5-fold in 12 week olds, and 2.4-fold in 18 week olds in comparison to 4 week olds. 4F4 expression dropped precipitously with age such that the levels were hardly detectable after 4 weeks. Similarly by 12 weeks of age, 4F5 levels had decreased compared to 4 weeks but the level of drop was much smaller as compared to 4F4. As seen in WKY, line SHR-B2 animals also showed increased 4F6 mRNA levels at 8 and 12 weeks of age but

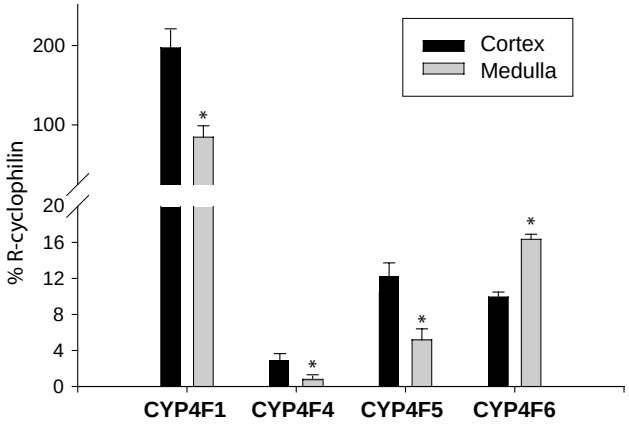

Fig. 3. Regional distribution of CYP4F isoforms in renal cortex and medulla. Total RNA was prepared from carefully dissected cortex or medulla from the rat kidneys ($n = 4$) and assayed for CYP4F expression using QRTPCR. Each sample was normalized to r-cyclophilin. Values are expressed as means ± SE. $^{*}P < 0.05$.

the expression was reduced back to 4 weeks levels at 18 weeks of age.

SHR-C

Rats from this sub-strain displayed the highest increase in CYP4F1 expression with respect to age. In this sub-strain, a 4.2-, 3.6-, and 4.1-fold rise in 4F1 expression from 4 weeks was observed at 8, 12, and 18 weeks. Although 4F4 expression at 4 weeks was the highest among all strains, there was once again a sharp decline in its relative levels throughout development. 4F5 showed a similar expression profile like 4F4 with a high expression detected early during development followed by a gradual loss with growth. On the contrary, 4F6 levels increased by 3-fold at 8 weeks from 4 weeks, but this increase started to fall as the animals grew older.

SHR-A3

As in two other SHR sub-strains, CYP4F1 levels in A3 also increased with age. After 4 weeks, 3-, 3.6-, and 3.2-fold rise in 4F1 expression was seen at 8, 12, and 18 weeks, respectively. Interestingly, 4F4 expression in SHR-A3 animals showed a slightly different profile similar to that observed in WKY animals. The expression levels initially increased by 2.9-fold at 8 weeks. This was followed by a large decline later during development. In contrast, CYP4F5 was observed to be at its minimal level around 8–12 weeks of age. CYP4F6 gene expression in SHR-A3 animals differed from the other SHR sub-strains and was fairly constant throughout development.

Comparative expression of CYP4F isoforms in normotensive and hypertensive rats

In all three SHR sub-strains, CYP4F1 mRNA levels in 4 week olds were nearly 2-fold lower than their WKY counterparts (Fig. 4). However, while 4F1 expression in WKY rats remained stable at all ages, the levels were significantly higher in all three sub-strains of SHR relative to age-matched WKY rats. From 8 to 18 weeks 4F1 displayed 1.5–1.7- fold difference between WKY and B2. The fold difference between WKY and C ranged from 1.5 to 2.3

Table 1
Age-related expression of Rat CYP4Fs in WKY and three substrains B2, C, and A3 of SHR

	Mean ± SE (% r-cyc)			
	CYP4F1	CYP4F4	CYP4F5	CYP4F6
WKY				
4-week-old	55.9 ± 8.39	0.214 ± 0.011	3.64 ± 0.27	7.16 ± 0.48
8-week-old	38.2 ± 3.02	0.583 ± 0.023**	3.52 ± 0.49	10.1 ± 0.78*
12-week-old	52.2 ± 8.29	0.0031 ± 0.0004**	1.85 ± 0.82	28.9 ± 6.19*
18-week-old	42.2 ± 3.44	0.0061 ± 0.0003**	1.64 ± 0.33**	6.85 ± 0.67
Line B2				
4-week-old	29.9 ± 3.04	0.287 ± 0.017	2.96 ± 0.72	9.38 ± 1.25
8-week-old	65.9 ± 2.78**	0.0007 ± 0.0003**	2.06 ± 0.69	17.3 ± 4.07
12-week-old	76.5 ± 6.63**	0.0031 ± 0.0004**	1.66 ± 0.38	17.7 ± 2.01*
18-week-old	72.1 ± 9.85*	0.0022 ± 0.0003**	1.65 ± 0.55	9.12 ± 1.07
Line C				
4-week-old	20.8 ± 1.09	0.522 ± 0.025	5.02 ± 0.14	8.93 ± 0.59
8-week-old	87.4 ± 6.99**	0.0005 ± 0.0002**	1.23 ± 0.15**	25.3 ± 5.68*
12-week-old	76.2 ± 11.1*	0.009 ± 0.002**	3.76 ± 0.87	15.7 ± 3.14
18-week-old	85.8 ± 0.98**	0.0051 ± 0.0011**	1.61 ± 0.38**	14.5 ± 1.85*
Line A3				
4-week-old	21.6 ± 2.58	0.371 ± 0.038	4.63 ± 0.66	12.5 ± 2.09
8-week-old	65.3 ± 10.5*	1.071 ± 0.131**	1.18 ± 0.19**	14.9 ± 3.49
12-week-old	77.9 ± 12.4*	0.0029 ± 0.0005**	1.45 ± 0.29**	9.89 ± 1.03
18-week-old	69.6 ± 7.37**	0.0035 ± 0.0008**	2.35 ± 0.35*	12.2 ± 1.01

QRTPCR assays were done in quadruplicate on the RNA prepared from WKY or SHR animals ($n = 4$) from different age groups. Data were analyzed and absolute values of mRNAs were generated by normalizing the copy number of each CYP4F to the copy number values of r-cyclophilin (internal standard). Data were analyzed using one-way ANOVA with statistical probabilities as $^{*}P < 0.05$, $^{**}P < 0.01$ in comparison to 4-week-old littermates.

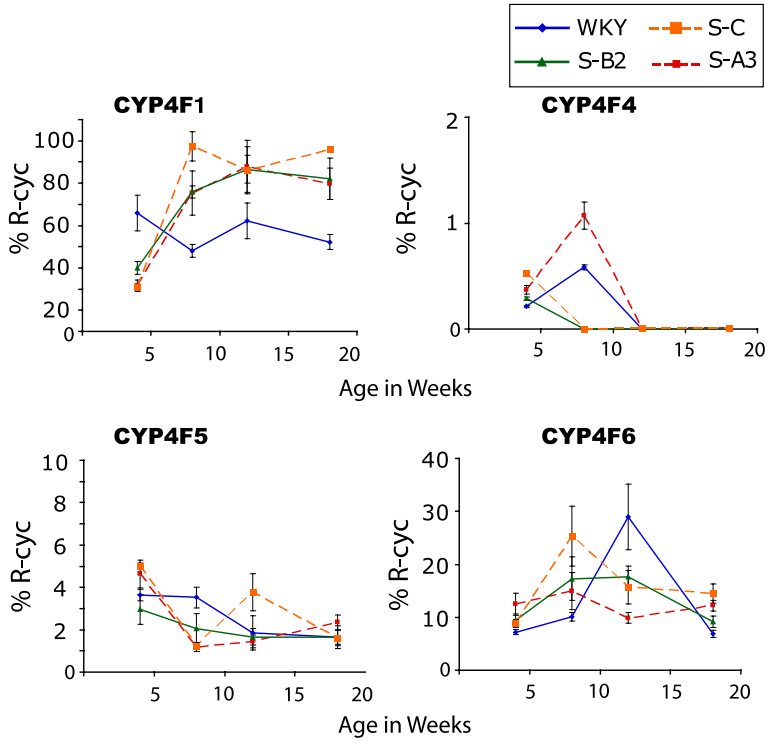

Fig. 4. QRTPCR analysis of CYP4F mRNA in WKY rat and three sub-strains of SHR. QRTPCR assays were done in quadruplicate on the RNA prepared from WKY or SHR animals ($n = 4$). All data were normalized to r-cyclophilin. Values are expressed as means ± SE.

and between WKY and A3 ranged from 1.5 to 1.7. The blood pressures of all three substrains of SHR were considerably higher in comparison to the WKY rats (Table 2).

In contrast to CYP4F1, 4F4 levels in SHR at 4 weeks were higher than WKY rats. At 8 weeks sub-strains B2 and C showed much lower 4F4 levels than WKY or sub-strain C (Fig. 4). Irrespective of the genetic background, 4F4 expression was highly suppressed after 12 weeks of age. 4F5 expression, on the other hand, varied among different SHR sub-strains but was not significantly different compared to their age-matched WKY rats. 4F6 levels like 4F4 were higher in SHR compared to WKY until 8 weeks. There was a sharp increase in 4F6 expression at 12 weeks in WKY rats while in the SHR there was a gradual loss of 4F6 gene expression. At 18 weeks 4F6 returned back to the 4 week levels in WKY rats and sub-strain B2 whereas in sub-strains C and A3 the levels remained similar as were at 12 weeks of age (Fig. 4).

Table 2
Systolic blood pressure recordings in three substrains of SHRs and WKY rats

Strain	Systolic BP
WKY	117 ± 1.4
SHR-B2	195 ± 2.0
SHR-C	177 ± 3.0
SHR-A3	199 ± 3.9

Blood pressures were determined by telemetry in 15–18-week-old SHR-A3 and WKY rats and by tail cuff in SHR-B2 (12 weeks of age) and SHR-C (9 weeks of age).

Discussion

CYP4Fs were previously cloned in our laboratory and their expression in liver and extrahepatic tissues was shown [21,29–31]. Little is known regarding the regional distribution of renal CYP4Fs, enzymes thought to be critical in 20-HETE production [20]. The goal of the present study was to examine the renal distribution and localization of CYP4F isoforms to correlate their distributions with their putative roles in physiological and pathophysiological processes. In particular, CYP4F gene expression was characterized to determine whether 4F renal expression was developmentally regulated in normal WKY and SHR rat strains.

It is not surprising that both CYP4F4 and 4F5 are evenly distributed in the liver, as are many other drug metabolism enzymes. This characteristic feature is largely due to the relative homogeneity of the liver. On the other hand, renal CYP4Fs were found to be preferentially localized in the cortex and outer medulla with the exception of CYP4F6. Thus, rat CYP4F distribution pattern matches the patterns seen with CYP4F2 and 4A11 in human kidney as reported by Lasker et al. [15]. They noted that CYP4F2 and 4A11 are both responsible for the formation of 20-HETE, a strong vasoconstrictor produced by kidney cortex microsomes with CYP4F2 being the major player in this process as compared to 4A11. Thus, in addition to LTB_4 metabolism [14,17,30,32], there is growing evidence for CYP4F-catalyzed AA metabolism strengthening the basis for their role in 20-HETE generation [16,17,20].

A recent comparison of kinetics of catalysis has revealed that the CYP4F subfamily is as efficient as the CYP4A subfamily in AA ω-hydroxylation [12]. Based on these observations, CYP4Fs were recognized as vital in regulating renal functions such as water–salt balance and blood pressure control. The results from the present study demonstrate CYP4F localization in cortical regions where the bulk of active absorption of salt and water takes place adding to the significance of CYP4Fs in pivotal renal functions in the presence or absence of inflammatory signals. Functional CYP ω-hydroxylase activity has been documented in the nephron and vasculature of the rat kidney, although it is not clear what percentage of this activity is due to CYP4A versus CYP4F isoforms. Detection of 20-HETE following addition of arachidonic acid to homogenates from microdissected nephrons indicates that functional arachidonic acid ω-hydroxylase activity is highest in the proximal tubules [33,34].

CYP4A and 4F isoforms are differentially distributed along the nephron in mice depending on sex and tubule segment including glomeruli [35]. Interestingly in the present study, intense CYP4F4 and 4F5 signals were observed in the cortex and outer medullary regions where proximal tubules are located whereas no CYP4F4 or 4F5 expression was seen in the glomeruli by in situ hybridization. Whether CYP4F1 or 4F6 is expressed in glomeruli is unclear at the present and remains to be characterized. The detection of AA ω-hydroxylase activity has been localized to the proximal tubules, whereas AA ω-1-hydroxylation is more widespread throughout the nephron [34]. Also, 20-HETE causes vasoconstriction of renal arteries and is therefore considered pro-hypertensive while its natriuretic and diuretic effects on renal tubules favor lowering of blood pressure. This suggests that the actual purpose of CYP4F isoforms in blood pressure regulation might be a function of their expression pattern within renal tubules and microvessels. Thus, localization of CYP4Fs along the nephron to more discrete regions might prove useful in discerning the relative importance of this subfamily in kidney function compared to CYP4As which are highly expressed in the S2 and S3 fragments of proximal tubules but are rare in the cortical collecting, distal convoluted, and connecting tubules [8].

Recently, mouse CYP4A isoforms were shown to play a part in male specific hypertension indicating a relationship between blood pressure regulation, sex hormones, and CYP ω-hydroxylases [36]. Targeted disruption of the CYP4A14 gene, instead of decreasing renal 20-HETE production, led to enhanced production of 20-HETE in the kidney and hypertension in male mice [36]. The increased 20-HETE production in these mice was attributed to an increase in the expression of the CYP4A12 isoform; however, changes in the expression of CYP4F isoforms were not considered in that study. Sex-dependent expression of CYP4Fs in the kidney is not unique to the mouse since rat 4Fs also exhibit sexually dimorphic expression in the liver, kidney, lung, and brain [21]. We have previously shown that renal CYP4F expression is regulated by estrogen in females [21]. This is in contrast to CYP4A expression, which is higher in males than females [37,38]. This would support a differential role for the CYP4F and CYP4A isoforms in 20-HETE formation in males and females.

Furthermore, to investigate the possibility of developmentally regulated CYP4F expression, we characterized the 4F gene expression with regard to age. Individual patterns of expression were observed for individual CYP4F isoforms in WKY and three SHR substrains. Each CYP4F gene was moderately expressed by 4 weeks of age in WKY or SHR kidney. Interestingly, CYP4F4 and 4F5 levels are tightly regulated during development with high expression seen through 8 weeks followed by a sharp decrease that persists through adulthood. This suggests that CYP4F4 and 4F5 might be important early in development. Recombinant CYP4F4 protein has been shown to be highly active in 20-HETE formation as well as in LTB_4 breakdown while specific activity for 4F5 is still a matter of discussion [20,30]. Although Kawashima et al. and Xu et al. [20,30] detected minor LTB_4 hydroxylation by CYP4F5 expressed in *E. coli*, Bylund et al. [32] were able to show extensive side-chain hydroxylation of LTB_4 by 4F5 expressed in yeast. A possible reason for this discrepancy could be the difference in the expression systems wherein the yeast-expressed CYP4F5 may undergo post-translational modifications that are absent in bacteria. Also, the need to determine the optimal reaction conditions for reconstitution of recombinant CYP4Fs can be another important factor for this discrepancy.

CYP4F4 has the highest arachidonic acid ω-hydroxylase activity [20] but its low expression seen in mature kidney does not support a major role for this isoform in renal 20-HETE formation during adulthood. It will be interesting to examine whether CYP4F4 contributes to 20-HETE biosynthesis in other tissues particularly lungs where 4F1 is absent. Also, we observed that CYP4F6 shows a significant increase around 8–12 weeks in WKY rats as well as in B2 and C substrains of SHR but by 18 weeks of age CYP4F6 levels drop back to the levels observed at 4 weeks. The current data suggest that CYP4F6 could be developmentally vital around 8–12 weeks but its exact function in development remains elusive at this time. Besides LTB_4 hydroxylation [32], 4F6 is also capable of metabolizing imipramine [39] but is not involved in AA ω-hydroxylation [20]. The CYP4F subfamily is also involved in metabolizing prostaglandins, lipoxins, tocopherol, HETE, and some clinically active drugs [14,40–42]; therefore, testing the catalytic capacity of CYP4F6 against these substrates might shed light on its endogenous functions.

In contrast to other CYP4F isoforms, CYP4F1 showed a steady increase in renal expression with age in all three substrains of SHR but not in WKY rats. This correlates well with increased 20-HETE levels and elevated blood pressure seen in these animals. Blood pressure becomes elevated in SHR compared to WKY rats from 5 weeks of age

and remains elevated thereafter [43]. Differences in AA ω-hydroxylation activity in renal microsomes from SHR and WKY rats have been known for several years [25–27,44]; however, altered CYP4A expression in the SHR is not completely coincident with the increased blood pressure. Increased expression of CYP4A3 and 4A8 has been suggested to be critical to the early changes in the eicosanoid formation and renal function in the young spontaneously hypertensive rat [9]. Since CYP4F1 is one of the major catalysts for 20-HETE biosynthesis [20] and we find it to be consistently upregulated in SHR compared to WKY rats, we speculate that 4F1 may be a critical enzyme in the development of hypertension in the spontaneously hypertensive rat.

Acknowledgments

The authors acknowledge the support by NIH Grants NS44174 and MH58927 to Henry W. Strobel and by President's Scholarship awarded to Auinash Kalsotra. The authors are thankful to Michael R. Blackburn for his collegial assistance.

References

[1] M.L. Schwartzman, P. Martasek, A.R. Rios, R.D. Levere, K. Solangi, A.I. Goodman, N.G. Abraham, Cytochrome P450-dependent arachidonic acid metabolism in human kidney, Kidney Int. 37 (1990) 94–99.
[2] J.D. Imig, A.P. Zou, D.E. Stec, D.R. Harder, J.R. Falck, R.J. Roman, Formation and actions of 20-hydroxyeicosatetraenoic acid in rat renal arterioles, Am. J. Physiol. 270 (1996) R217–R227.
[3] A.P. Zou, J.T. Fleming, J.R. Falck, E.R. Jacobs, D. Gebremedhin, D.R. Harder, R.J. Roman, 20-HETE is an endogenous inhibitor of the large-conductance Ca(2+)-activated K^+ channel in renal arterioles, Am. J. Physiol. 270 (1996) R228–R237.
[4] M. Schwartzman, N.R. Ferreri, M.A. Carroll, E. Songu-Mize, J.C. McGiff, Renal cytochrome P450-related arachidonate metabolite inhibits (Na+ + K+)ATPase, Nature 314 (1985) 620–622.
[5] B. Escalante, D. Erlij, J.R. Falck, J.C. McGiff, Effect of cytochrome P450 arachidonate metabolites on ion transport in rabbit kidney loop of Henle, Science 251 (1991) 799–802.
[6] A.P. Zou, J.D. Imig, P.R. Ortiz de Montellano, Z. Sui, J.R. Falck, R.J. Roman, Effect of P-450 omega-hydroxylase metabolites of arachidonic acid on tubuloglomerular feedback, Am. J. Physiol. 266 (1994) F934–F941.
[7] Y.H. Ma, D. Gebremedhin, M.L. Schwartzman, J.R. Falck, J.E. Clark, B.S. Masters, D.R. Harder, R.J. Roman, 20-Hydroxyeicosatetraenoic acid is an endogenous vasoconstrictor of canine renal arcuate arteries, Circ. Res. 72 (1993) 126–136.
[8] M.L. Schwartzman, J.L. da Silva, F. Lin, M. Nishimura, N.G. Abraham, Cytochrome P450 4A expression and arachidonic acid omega-hydroxylation in the kidney of the spontaneously hypertensive rat, Nephron 73 (1996) 652–663.
[9] D.L. Kroetz, L.M. Huse, A. Thuresson, M.P. Grillo, Developmentally regulated expression of the CYP4A genes in the spontaneously hypertensive rat kidney, Mol. Pharmacol. 52 (1997) 362–372.
[10] P. Su, K.M. Kaushal, D.L. Kroetz, Inhibition of renal arachidonic acid omega-hydroxylase activity with ABT reduces blood pressure in the SHR, Am. J. Physiol. 275 (1998) R426–R438.
[11] D.E. Stec, A.Y. Deng, J.P. Rapp, R.J. Roman, Cytochrome P4504A genotype cosegregates with hypertension in Dahl S rats, Hypertension 27 (1996) 564–568.
[12] D.L. Kroetz, F. Xu, Regulation and inhibition of arachidonic acid—hydroxylases and 20-HETE formation, Annu. Rev. Pharmacol. Toxicol. (2004).
[13] R.T. Okita, J.R. Okita, Cytochrome P450 4A fatty acid omega hydroxylases, Curr. Drug Metab. 2 (2001) 265–281.
[14] Y. Kikuta, E. Kusunose, M. Kusunose, Prostaglandin and leukotriene omega-hydroxylases, Prostaglandins Other Lipid Mediat. 68–69 (2002) 345–362.
[15] J.M. Lasker, W.B. Chen, I. Wolf, B.P. Bloswick, P.D. Wilson, P.K. Powell, Formation of 20-hydroxyeicosatetraenoic acid, a vasoactive and natriuretic eicosanoid, in human kidney. Role of Cyp4F2 and Cyp4A11, J. Biol. Chem. 275 (2000) 4118–4126.
[16] P.K. Powell, I. Wolf, R. Jin, J.M. Lasker, Metabolism of arachidonic acid to 20-hydroxy-5,8,11,14-eicosatetraenoic acid by P450 enzymes in human liver: involvement of CYP4F2 and CYP4A11, J. Pharmacol. Exp. Ther. 285 (1998) 1327–1336.
[17] P. Christmas, J.P. Jones, C.J. Patten, D.A. Rock, Y. Zheng, S.M. Cheng, B.M. Weber, N. Carlesso, D.T. Scadden, A.E. Rettie, R.J. Soberman, Alternative splicing determines the function of CYP4F3 by switching substrate specificity, J. Biol. Chem. 276 (2001) 38166–38172.
[18] U. Hoch, Z. Zhang, D.L. Kroetz, P.R. Ortiz de Montellano, Structural determination of the substrate specificities and regioselectivities of the rat and human fatty acid omega-hydroxylases, Arch. Biochem. Biophys. 373 (2000) 63–71.
[19] X. Nguyen, M.H. Wang, K.M. Reddy, J.R. Falck, M.L. Schwartzman, Kinetic profile of the rat CYP4A isoforms: arachidonic acid metabolism and isoform-specific inhibitors, Am. J. Physiol. 276 (1999) R1691–R1700.
[20] F. Xu, J.R. Falck, P.R. Ortiz de Montellano, D.L. Kroetz, Catalytic activity and isoform-specific inhibition of rat cytochrome p450 4F enzymes, J. Pharmacol. Exp. Ther. 308 (2004) 887–895.
[21] A. Kalsotra, S. Anakk, C.L. Boehme, H.W. Strobel, Sexual dimorphism and tissue specificity in the expression of CYP4F forms in Sprague–Dawley rats, Drug Metab. Dispos. 30 (2002) 1022–1028.
[22] K. Okamoto, K. Aoki, Development of a strain of spontaneously hypertensive rats, Jpn. Circ. J. 27 (1963) 282–293.
[23] A. Nagaoka, H. Iwatsuka, Z. Suzuoki, K. Okamoto, Genetic predisposition to stroke in spontaneously hypertensive rats, Am. J. Physiol. 230 (1976) 1354–1359.
[24] B. Gigante, S. Rubattu, R. Stanzione, A. Lombardi, A. Baldi, F. Baldi, M. Volpe, Contribution of genetic factors to renal lesions in the stroke–prone spontaneously hypertensive rat, Hypertension 42 (2003) 702–706.
[25] K. Omata, N.G. Abraham, B. Escalante, M.L. Schwartzman, Age-related changes in renal cytochrome P-450 arachidonic acid metabolism in spontaneously hypertensive rats, Am. J. Physiol. 262 (1992) F8–F16.
[26] J.D. Imig, J.R. Falck, D. Gebremedhin, D.R. Harder, R.J. Roman, Elevated renovascular tone in young spontaneously hypertensive rats. Role of cytochrome P-450, Hypertension 22 (1993) 357–364.
[27] D.E. Stec, M.R. Trolliet, J.E. Krieger, H.J. Jacob, R.J. Roman, Renal cytochrome P4504A activity and salt sensitivity in spontaneously hypertensive rats, Hypertension 27 (1996) 1329–1336.
[28] P. Chomczynski, A reagent for the single-step simultaneous isolation of RNA, DNA and proteins from cell and tissue samples, Biotechniques 15 (1993) 532–534, 536–537.
[29] H. Kawashima, H.W. Strobel, cDNA cloning of three new forms of rat brain cytochrome P450 belonging to the CYP4F subfamily, Biochem. Biophys. Res. Commun. 217 (1995) 1137–1144.
[30] H. Kawashima, E. Kusunose, C.M. Thompson, H.W. Strobel, Protein expression, characterization, and regulation of CYP4F4 and CYP4F5 cloned from rat brain, Arch. Biochem. Biophys. 347 (1997) 148–154.
[31] A. Kalsotra, X. Cui, L. Antonovic, A.M. Robida, E.T. Morgan, H.W. Strobel, Inflammatory prompts produce isoform-specific changes in the expression of leukotriene B(4) omega-hydroxylases in rat liver and kidney, FEBS Lett. 555 (2003) 236–242.

[32] J. Bylund, A.G. Harder, K.G. Maier, R.J. Roman, D.R. Harder, Leukotriene B4 omega-side chain hydroxylation by CYP4F5 and CYP4F6, Arch. Biochem. Biophys. 412 (2003) 34–41.
[33] F. Lin, N.G. Abraham, M.L. Schwartzman, Cytochrome P450 arachidonic acid omega-hydroxylation in the proximal tubule of the rat kidney, Ann. NY Acad. Sci. 744 (1994) 11–24.
[34] K. Omata, N.G. Abraham, M.L. Schwartzman, Renal cytochrome P-450-arachidonic acid metabolism: localization and hormonal regulation in SHR, Am. J. Physiol. 262 (1992) F591–F599.
[35] D.E. Stec, A. Flasch, R.J. Roman, J.A. White, Distribution of cytochrome P-450 4A and 4F isoforms along the nephron in mice, Am. J. Physiol. Renal. Physiol. 284 (2003) F95–F102.
[36] V.R. Holla, F. Adas, J.D. Imig, X. Zhao, E. Price Jr, N. Olsen, W.J. Kovacs, M.A. Magnuson, D.S. Keeney, M.D. Breyer, J.R. Falck, M.R. Waterman, J.H. Capdevila, Alterations in the regulation of androgen-sensitive Cyp 4a monooxygenases cause hypertension, Proc. Natl. Acad. Sci. USA 98 (2001) 5211–5216.
[37] B. Jeffery, A.I. Choudhury, N. Horley, M. Bruce, S.R. Tomlinson, R.A. Roberts, T.J. Gray, D.A. Barrett, P.N. Shaw, D. Kendall, D.R. Bell, Peroxisome proliferator activated receptor alpha regulates a male-specific cytochrome P450 in mouse liver, Arch. Biochem. Biophys. 429 (2004) 231–236.
[38] S.R. Mitchell, M.B. Sewer, S.S. Kardar, E.T. Morgan, Characterization of CYP4A induction in rat liver by inflammatory stimuli: dependence on sex, strain, and inflammation-evoked hypophagia, Drug Metab. Dispos. 29 (2001) 17–22.
[39] H. Kawashima, D.J. Sequeira, D.R. Nelson, H.W. Strobel, Genomic cloning and protein expression of a novel rat brain cytochrome P-450 CYP2D18* catalyzing imipramine N-demethylation, J. Biol. Chem. 271 (1996) 28176–28180.
[40] T.J. Sontag, R.S. Parker, Cytochrome P450 omega-hydroxylase pathway of tocopherol catabolism. Novel mechanism of regulation of vitamin E status, J. Biol. Chem. 277 (2002) 25290–25296.
[41] A. Kalsotra, C.M. Turman, Y. Kikuta, H.W. Strobel, Expression and characterization of human cytochrome P450 4F11: putative role in the metabolism of therapeutic drugs and eicosanoids, Toxicol. Appl. Pharmacol. 199 (2004) 295–304.
[42] T. Hashizume, S. Imaoka, M. Mise, Y. Terauchi, T. Fujii, H. Miyazaki, T. Kamataki, Y. Funae, Involvement of CYP2J2 and CYP4F12 in the metabolism of ebastine in human intestinal microsomes, J. Pharmacol. Exp. Ther. 300 (2002) 298–304.
[43] W.H. Beierwaltes, W.J. Arendshorst, P.J. Klemmer, Electrolyte and water balance in young spontaneously hypertensive rats, Hypertension 4 (1982) 908–915.
[44] S. Imaoka, Y. Funae, Hepatic and renal cytochrome P-450s in spontaneously hypertensive rats, Biochim. Biophys. Acta 1074 (1991) 209–213.